Author Manuscript

Author Manuscript

Author Manuscript

Author Manuscript

HHS Public Access

Author manuscript

Vasc Med. Author manuscript; available in PMC 2021 June 25.

Published in final edited form as:

Vasc Med. 2021 June ; 26(3): 247–258. doi:10.1177/1358863X20983918.

Racial differences in the limb skeletal muscle transcriptional programs of patients with critical limb ischemia

Zoe S Terwilliger[1,2], **Terence E Ryan**[3], **Emma J Goldberg**[1,2], **Cameron A Schmidt**[1,2], **Dean J Yamaguchi**[4,5], **Reema Karnekar**[1,2], **Patricia Brophy**[1], **Thomas D Green**[1,2], **Tonya N Zeczycki**[1,6], **Feilim Mac Gabhann**[7], **Brian H Annex**[8,9], **Joseph M McClung**[1,2,4]

[1]Diabetes and Obesity Institute, East Carolina University, Brody Medical Center, Greenville, NC, USA

[2]Department of Physiology, East Carolina University, Brody Medical Center, Greenville, NC, USA

[3]Department of Applied Physiology and Kinesiology, University of Florida, Gainesville, FL, USA

[4]Department of Cardiovascular Sciences, East Carolina University, Brody Medical Center, Greenville, NC, USA

[5]Division of Surgery, East Carolina University, Brody Medical Center, Greenville, NC, USA

[6]Department of Biochemistry, East Carolina University, Brody Medical Center, Greenville, NC, USA

[7]Department of Biomedical Engineering and Institute for Computational Medicine, Johns Hopkins School of Medicine, Baltimore, MD, USA

[8]Department of Medicine, Medical College of Georgia, Augusta, GA, USA

[9]Vascular Biology Center, Medical College of Georgia, Augusta, GA, USA

Abstract

Critical limb ischemia (CLI) is the most severe manifestation of peripheral artery disease (PAD) and is characterized by high rates of morbidity and mortality. As with most severe cardiovascular disease manifestations, Black individuals disproportionately present with CLI. Accordingly, there remains a clear need to better understand the reasons for this discrepancy and to facilitate personalized therapeutic options specific for this population. Gastrocnemius muscle was obtained from White and Black healthy adult volunteers and patients with CLI for whole transcriptome shotgun sequencing (WTSS) and enrichment analysis was performed to identify alterations in specific Reactome pathways. When compared to their race-matched healthy controls, both White and Black patients with CLI demonstrated similar reductions in nuclear and mitochondrial encoded genes and mitochondrial oxygen consumption across multiple substrates, indicating a common bioenergetic paradigm associated with amputation outcomes regardless of race. Direct

Article reuse guidelines: sagepub.com/journals-permissions

Corresponding author: Joseph M McClung, Diabetes and Obesity Institute, East Carolina Heart Institute, Brody School of Medicine at East Carolina University, Office #4109, Mail Stop 743, 115 Heart Drive, Greenville, NC 27834-4354, USA. mcclungj@ecu.edu.

Declaration of conflicting interests

The authors declared no potential conflicts of interest with respect to the research, authorship, and/or publication of this article.

Author Manuscript Author Manuscript Author Manuscript Author Manuscript

comparisons between tissues of White and Black patients with CLI revealed hemostasis, extracellular matrix organization, platelet regulation, and vascular wall interactions to be uniquely altered in limb muscles of Black individuals. Among traditional vascular growth factor signaling targets, WTSS revealed only *Tie1* to be significantly altered from White levels in Black limb muscle tissues. Quantitative reverse transcription polymerase chain reaction validation of select identified targets verified WTSS directional changes and supports reductions in *MMP9* and increases in *NUDT4P1* and *GRIK2* as unique to limb muscles of Black patients with CLI. This represents a critical first step in better understanding the transcriptional program similarities and differences between Black and White patients in the setting of amputations related to CLI and provides a promising start for therapeutic development in this population.

Keywords

critical limb ischemia (CLI); genetics; health disparities; ischemia; mitochondria; peripheral artery disease (PAD); skeletal muscle

Introduction

The paucity of therapeutic advances for peripheral artery disease (PAD) over the last 20 years is of great concern, given the aging of the general population and collective prevalence of primary risk factors such as diabetes and other cardiovascular diseases.[1] Symptomatic PAD presents as either intermittent claudication (IC; pain with exertion that is relieved with rest) or critical limb ischemia (CLI; pain at rest with or without tissue necrosis or gangrene). Patients with CLI have a risk of major amputation or death, and many patients that fall into this category are not amenable to surgical or catheter-based revascularization as these invasive procedures carry a significant risk (i.e. heart attack or kidney failure). Like other cardiovascular diseases, CLI disproportionately affects Black populations. Even after adjustment for other causes, the odds for incident PAD and death in Black patients are 1.67 times and 5% higher (per 100,000), respectively, than for White patients (for review, see[2]). In fact, neither disparities in risk factors nor access to care adequately explain the prevalence of PAD in Black patients.[2,3] There is unfortunately very little progress made towards identifying proven strategies to improve limb perfusion and tissue salvage in patients with CLI. This creates a log-jam effect in the development of specific therapeutic avenues for a suffering population of Black patients with PAD.

While the cause of PAD is occlusive atherosclerosis of the large arteries, the ischemic events produced by the occlusive disease contribute to a myriad of alterations in the downstream tissues. In the case of the peripheral limb, skeletal muscle is a strong predictor of morbidity and mortality in patients[4] and undergoes a unique transcriptional profile change in patients with CLI. There exists a twofold greater incidence of PAD in the Black community than the White population;[5] however, reasons for this discrepancy remain obscure. While progress is beginning to be made to better understand the greater CLI population as a whole, distinct analyses of how race alters patient tissue biology are sparse. The purpose of this study was to examine whether unified transcriptional programs linked White and Black CLI patient skeletal muscles in comparison to race-matched controls, and to further determine whether a

Author Manuscript Author Manuscript Author Manuscript Author Manuscript

unique transcriptional program existed specifically in the amputated limb muscle of Black patients with CLI. Our data provide a yet unseen characterization of unique transcriptome changes in the target tissues (limb skeletal muscles) of Black patients with CLI. While race-independent similarities in tissues exist at the time of amputation in patients with CLI, including consistent and pervasive deficits in the skeletal muscle oxidative metabolism profile, there are tangible and consistent differences in the limb muscle transcriptional program that differentiate the tissues of Black patients from White patients. This represents a critical first step in better understanding the unique local microenvironment present in Black CLI limb muscles and provides a promising direction for therapeutic investigation of these patients.

Methods

Study approval

This study was approved by the institutional review board at East Carolina University (Greenville, NC, USA) and was carried out in accordance with the Declaration of Helsinki. All participants gave written informed consent prior to enrollment.

Study participants

Nineteen patients with CLI were recruited through print advertising or identified by vascular surgeons at East Carolina University (ECU) Brody Medical Center. These patients were part of a broader study of PAD previously described.[6] The following analysis was designed to specifically examine patients representative of the CLI classification of PAD whose disease culminated in the need for amputation (above- or below-knee) regardless of previous revascularization procedures, as indicated in the patient physical and clinical characteristics shown in Table 1. Exclusion criteria consisted only of secondary enrollment of CLI amputation patients who previously provided biological specimens from the contralateral limb. Healthy adult (HA) patients volunteered for tissue biopsy and self-reported as symptom- and diagnosis-free. All data collection was carried out by blinded investigators at ECU. For the purposes of this study, and since detailed patient genealogy was not available at the time of enrollment, Black is the designation for all Black patients that were received and treated by the Vascular Surgery Department in Eastern North Carolina at ECU-Brody School of Medicine, regardless of country of origin. Similarly, White is the designation for all White patients, regardless of country of origin. Race data were collected as self-identified by the patients in the clinic.

RNA isolation and transcriptome sequencing

Total RNA was extracted using Qiagen RNeasy Midi Kits per manufacturer instructions (Germantown, MD, USA). RNA sequencing was performed as described previously in detail[6] by Quick Biology Inc. (Pasadena, CA, USA). RNA integrity was checked by Agilent Bioanalyzer 2100 (Santa Clara, California, USA); only samples with clean rRNA peaks were used. The library for RNA-Seq was prepared according to KAPA Stranded mRNA-Seq poly(A) selected kit with 201–300 bp insert size (KAPA Biosystems, Wilmington, MA, USA) using 250 ng total RNA as input. Final library quality and quantity was analyzed by Agilent Bioanalyzer 2100 and Life Technologies Qubit 3.0 Fluorometer (Carlsbad,

Author Manuscript Author Manuscript Author Manuscript Author Manuscript

California, USA). The 150 bp paired end reads were sequenced on Illumina HighSeq 4000 (Illumnia Inc., San Diego, CA, USA). The reads were first mapped to the latest University of California Santa Cruz transcript set using Bowtie2 version 2.1.0 and the gene expression level was estimated using RSEM v1.2.15. TMM (trimmed mean of M-values) was used to normalize the gene expression. Differentially expressed genes were identified using the edgeR program. Genes showing altered expression with $p < 0.05$ and more than 1.5-fold changes were considered differentially expressed. GOseq was used to perform a gene ontology (GO) enrichment analysis and Reactome (https://reactome.org) was used to perform the Reactome analysis specific for this work. Heatmaps were generated with Prism program using a $\log_2$ (fold change from non-PAD or C CLI). To further validate RNA-seq findings, RNA was reverse transcribed using Superscript IV Reverse Transcriptase according to manufacturer instructions (Invitrogen; Carlsbad, CA, USA). Real-time polymerase chain reaction (RT-PCR) on selected gene targets was performed using a QuantStudio 3 Real-Time PCR system (Applied Biosystems, Foster City, CA, USA). Relative quantification of mRNA levels was determined using the comparative threshold cycle (DDCT) method using FAM-labeled Taqman Gene expression assays (Applied Biosystems) specific to the given gene run in multiplex with a VIC-labeled 18S control primer.

Preparation of permeabilized muscle fibers

A portion of each muscle sample was immediately placed in ice-cold buffer X (50 mM K-MES, 7.23 mM K_2EGTA, 2.77 mM CaK_2EGTA, 20 mM imidazole, 20 mM taurine, 5.7 mM ATP, 14.3 mM phosphocreatine, and 6.56 mM $MgCl_2$-$6H_2O$, pH 7.1) for preparation of permeabilized fiber bundles (PmFBs) as previously described[7]. Fiber bundles were separated along their longitudinal axis using needle-tipped forceps under magnification (MX6 Stereoscope; Leica Microsystems, Buffalo Grove, IL, USA), permeabilized with saponin (30 μg/mL) for 30 minutes at 4°C on a nutating mixer, and subsequently washed in cold buffer Z (105 mM K-MES, 30 mM KCl, 1 mM EGTA, 10 mM K_2HPO_4, 5 mM $MgCl_2$-$6H_2O$, 0.5 mg/mL BSA, pH 7.1) for 15 minutes until analysis. At the conclusion of each experiment, PmFBs were washed in double-distilled H_2O to remove salts, freeze-dried (Labconco; Kansas City, MO, USA), and weighed. Typical fiber bundle sizes were 0.2–0.6 mg dry weight.

Mitochondrial respiration measurements

High-resolution O_2 consumption measurements[7] were conducted at 37°C in Buffer Z (in mmol/L) (105 K-MES, 30 KCl, 1 EGTA, mM K_2HPO_4, 5 $MgCl_26H_2O$, 0.5 mg/mL BSA, pH 7.1), supplemented with creatine monohydrate (20 mM), using the Oroboros O2k Oxygraph (Innsbruck, Austria). A substrate inhibitor titration protocol was performed as follows: 2 mmol/L malate + 10 mmol/L glutamate (State 2 respiration), followed by the addition of 4 mmol/L ADP to initiate state 3 respiration supported by Complex I substrates. Convergent electron flow through Complexes I and II was initiated with the addition of 10 mmol/L succinate. Rotenone (10 μmol/L) was subsequently added to inhibit Complex I, followed by 10 μmol/L cytochrome *c* to test the integrity of the mitochondrial membrane. Complex IV-supported respiration was examined using the electron donor *N,N,N',N'*-tetramethyl-*p*-phenylenediamine (TMPD) at 0.4 mmol/L in the presence of 2 mmol/L ascorbate (to limit auto-oxidation of TMPD) and 5 μmol/L antimycin A (to prevent reverse

Author Manuscript Author Manuscript Author Manuscript Author Manuscript

electron flow through Complex III). The rate of respiration was expressed as pmol/s/mg fiber dry weight. All respiration measurements were conducted at 37°C and a working range (O_2) of ~350 to 200 μM.

Citrate synthase activity

Activity assays were performed using a citrate synthase activity assay kit (Sigma CS0720, St. Louis, MO, USA) per the manufacturer's instructions. Briefly, skeletal muscles or primary myotube lysates were generated by glass pestle homogenization by hand in RIPA buffer. Protein concentrations were determined using a BCA Protein Assay (Pierce Thermo Fisher #23225, Waltham, MA, USA). Activity assays were performed in assay buffer containing (in mmol/L): 100 Tris, 1 EDTA, 1 EGTA, 10 DTNB (Sigma: D8130), and 30 Acetyl-CoA at pH 8.35. All samples were measured in duplicate and the average absorbance was used in final calculations of activity. Background absorbance was measured prior to addition of 10 mM oxaloacetate (Sigma: O4126) and final activity rates were corrected for those values.

Relative specific activity of mitochondrial OXPHOS complexes

Frozen skeletal muscle from the muscle biopsy procedure was homogenized in 0.3 M sucrose, 10 mM HEPES, 1 mM EGTA on ice[8], centrifuged at 800 for 10 min, and protein in the supernatant was quantified using the BCA protein assay kit (Life Technologies). Specific activities of all individual ETS complexes were determined spectrophotometrically as described in.[9] Briefly, aliquots of skeletal muscle lysates were diluted in hypotonic medium (25 mM K_2HPO_4, 5.3 mM $MgCl_2$, pH 7.2) and further subjected to three to four freeze–thaw cycles. Complex I activity was determined in 5 mM Tris, 0.5 mg/mL BSA, 24 μM KCN, 0.4 μM antimycin A, pH 8, following the oxidation of NADH (0.8 mM) at 340 nm (ε_{340} = 6220 M^{-1} cm^{-1}) for 3 min using oxidized decylubiquinone (50 μM DCU_{ox}) as the electron acceptor. Rotenone (4 μM) was added to measure rotenone-sensitive NADH-DCU oxidoreductase activity. Complex II activity was measured in SQR medium (10 mM KH_2PO_4, 2 mM EDTA, 1 mg/mL BSA) in the presence of 10 mM succinate, following the reduction of dichlorophenolindophenol (80 μM DCPIP) at 600 nm (ε_{340} = 19,100 M^{-1} cm^{-1}) for 3 min, using DCU_{ox} as the electron acceptor. The reaction was inhibited by the addition of the competitive substrate malonate (10 mM). Complex III activity was measured in SQR medium supplemented with 200 μM ATP, and 240 μM KCN, using DCU_{red} (80 mM) as the electron donor and oxidized cytochrome *c* as the acceptor (40 μM). The reaction was followed by measuring the reduction of cytochrome *c* at 550 nm (ε_{340} = 18,500 M^{-1} cm^{-1}) for 3 min, and finally inhibited by the addition of 0.5 μM myxothiazol. Cytochrome *c* oxidase (Complex IV) was determined with the addition of 1 mM reduced cytochrome *c* by following the decrease in absorbance at 550 nm. Potassium cyanide was added to check for the specificity of complex IV activity.

Skeletal muscle histology

Skeletal muscle morphology was assessed by standard light microscopy. Transverse sections of 10 μm thick from muscle biopsy samples of the gastrocnemius muscle frozen in liquid nitrogen-cooled isopentane in optimum mounting medium (OCT) were cut using a Leica 3050S cryotome (Leica Biosystems Inc., Buffalo Grove, IL, USA) and collected on charged

Author Manuscript Author Manuscript Author Manuscript Author Manuscript

slides for staining. For morphological analyses, standard methods for hematoxylin and eosin (H&E) histological staining were performed and images were acquired using an EVOS FL Auto widefield microscope (Life Technologies) with a plan-fluorite 20× cover-slip corrected objective (NA 0.5, air).

Immunofluorescence

CLI tissues were prepared as described above. CLI sections were fixed in 1:1 acetone/methanol for 10 min at −20°C and rehydrated in 1× PBS. All sections were blocked in 5% goat serum + 1× PBS for 1 h at room temperature. For dystrophin immunofluorescence, sections were incubated with rabbit anti-human dystrophin primary antibody at 4°C overnight (1:100 dilution, Thermo Rb-9024; targeted to the protein C-terminus). Sections were washed 3× for 10 min with cold 1× PBS and incubated for 1 h with Alexa Fluor 488 conjugated anti-rabbit IgG secondary antibody (1:250; Invitrogen). For fiber typing analysis, sections were incubated with mouse anti-bovine myosin heavy chain (MyHC) type I (slow) (DSHB BA-D5) primary antibody at 4°C overnight (1:100 dilution). Sections were washed 3× for 10 min with cold 1× PBS. For dystrophin immunofluorescence, sections were incubated for 1 h with Alexa Fluor 488 conjugated anti-rabbi IgG1 secondary antibody (1:250; Invitrogen). For fiber typing, sections were incubated for 1 h with Alexa Fluor 594 conjugated goat anti-mouse IgG2b secondary antibodies (1:250; Invitrogen). Sections were mounted using Vectashield hard mount medium with DAPI (Vector Labs, Burlingame, CA, USA). Images were taken as described above.

Image processing

Image processing was performed using ImageJ (NIH, v1.49). All processing was performed uniformly over the entire image, and processing parameters were made constant for the entire image set. H&E-stained images were dark field corrected using a correction image collected at the time of acquisition. Corrections were performed using the image calculator plus plugin. Images were contrast enhanced with a 0.3% pixel saturation threshold. In order to facilitate feature enhancement in representative image panels where features may be obscured due to the small size of the images, an unsharp mask filter was applied to the dark field corrected/contrast enhanced H&E images (mask weight = 0.6; pixel radius = 1). No images used for quantification were altered from their original format prior to analysis. The muscle fiber cross-sectional area was measured by a blinded investigator. From each 4× magnification image, 200 fibers were measured, and samples were pooled for frequency distributions. From a test set of each type of patient sample, 200 fibers was determined as the minimum number of measurements required to achieve a stable variance among the measurements. Fiber type proportions were counted from two 4× magnification images from each sample.

Statistics

Data are presented as mean ± SEM. Statistical analyses were performed using GraphPad Software Prism, version 9 (GraphPad Software, San Diego, CA, USA). Comparisons between two groups were performed by Student’s two-tailed *t*-test. Comparisons of data with more than two groups were performed using two-way ANOVA with Tukey’s post hoc

Author Manuscript Author Manuscript Author Manuscript Author Manuscript

multiple comparisons. Repeated measures ANOVA was used when appropriate. In all cases, $p < 0.05$ was considered statistically significant.

Results

Our recent work within a group of patients with PAD revealed a unique transcriptional program in CLI limb muscles and specifically highlighted a unique bioenergetic signature versus either healthy control or claudication tissues.[6] Here, we set out to determine whether transcriptome differences existed within the same population between Black and White HA or patients with CLI. Patient characteristics from the subjects are presented in Table 1. The HA patient population self-reported as symptom- and diagnosis-free. The CLI population reported ischemic pain at rest. In the Black-CLI population, 78% of patients and 60% of White-CLI patients were diagnosed with a form of diabetes mellitus. In total, 67% of Black-CLI and 100% of White-CLI patients presented with hypertension, while only 33% and 20% reported hyperlipidemia, respectively. Five Black-CLI patients had renal disease compared with two in the White-CLI population. Eight Black-CLI and two White-CLI patients were former smokers. Five Black-CLI and three White-CLI patients reported a family history of coronary artery disease (CAD) with four of the Black-CLI patients diagnosed with CAD. The average ankle–brachial index (ABI) was 0.31 in Black patients with CLI and 0.43 in White patients, with nearly half of both patient populations presenting as non-compressible at the time of amputation. Of the Black and White patients with CLI, 44% and 60% had previously undergone a revascularization surgery, respectively.

Limb muscle transcriptome changes in White patients with CLI

Whole transcriptome shotgun sequencing (WTSS) analyses between limb skeletal muscle of White HA and White-CLI patients was first performed (Figure 1A,B) and revealed an upregulation of 2679 genes and a downregulation of 1450 genes in the White-CLI patients. Reactome analysis of the results (Figure 1C) individually highlighted cellular respiration, including genes involved in the citric acid cycle and electron transport, as prominent alterations in White patients. Other Reactome alterations of note were seen in White patients with CLI in the hemostasis, cellular interaction, and platelet activation categories. The 30 individual gene targets identified by greatest significance (p-value; either increased or decreased expression) are presented in Figure 1D. Matrix metallopeptidase-9 (*MMP9*), chitinase 2-like 1 (cartilage glycoprotein-39; *CHI3L1*), serum A1 (*SAA1*), and FBJ murine osteosarcoma viral oncogene homolog B (*FOSB*) presented the largest fold changes in the White-CLI group. Methyltransferase-like 21E, pseudogene (*METTL21EP*) was the only target identified to decrease in White patients with CLI to make the top 30 list of significance as determined by p-value.

Limb muscle transcriptome changes in Black patients with CLI

WTSS analyses were also used to examine limb skeletal muscle of Black HA patients and Black-CLI patients (Figure 2A,B) and revealed an upregulation of 2190 genes and a downregulation of 1660 genes in Black patients with CLI. Similar to the White patients with CLI, Reactome enrichment analysis (Figure 2C) revealed significant gene expression changes in genes involved in the citric acid cycle and electron transport as well as genes

Author Manuscript Author Manuscript Author Manuscript Author Manuscript

involved in ATP synthesis by chemiosmotic coupling. Other affected genes included those involved in extracellular matrix organization, mitochondrial translation, and mitochondrial DNA synthesis. Interestingly, the observed differences in the top 30 targets of the Black-CLI group (Figure 2D) included both increased and decreased gene targets, in contrast to the target list of White patients with CLI. The genes for collagen, type XIX, alpha 1 (*COL19A1*), cyclin-dependent kinase inhibitor (*CDKN1A*), and runt-related transcription factor 1 (*RUNX1*) had the greatest increased fold changes in the Black patients. The genes for methyltransferase-like 21E, pseudogene (*METTL21EP*) and long intergenic non-protein coding RNA 202–1 (*LINC00202–1*) demonstrated the largest decreased fold change in Black patients. The results of the Black individual gene targets show a larger variation of fold changes when compared with that of the White patients with CLI.

Decreased mitochondrial respiration is a race-independent component of CLI limb muscle

Muscle biopsy samples were uniformly collected from the gastrocnemius muscle (10 cm distal to the tibial tuberosity) of both White and Black patients with CLI undergoing limb amputation. Histological (H&E) and dystrophin staining confirmed intact muscle architecture (Figure 3A), similar myofiber cross-sectional areas (Figure 3B), and similar proportions of Type 1 fibers (Figure 3C), ensuring that transcriptome alterations of racial groups were not overtly influenced by necrosis or phenotypic differences in the biopsy specimens. We performed secondary analysis of our comprehensive mitochondrial phenotyping experiments performed using permeabilized myofibers and multiple substrate high-resolution respirometry[6] specifically to determine whether mitochondria from Black patients with CLI function differentially from White. Mitochondrial respiratory capacity in myofiber bundles from Black patients was not statistically different from White patients' muscle across a multiple substrate platform (Figure 3D), which is an important finding linking mitochondrial insufficiency to amputation outcome regardless of race/ethnicity. Patient limb muscle mitochondrial number/density, assessed using citrate synthase activity, revealed similar mitochondrial content (Figure 3E). Specific activities of the respiratory Complexes I, II, III, and IV were next determined spectrophotometrically in muscle homogenates to further characterize changes in mitochondrial respiration (Figure 3F–I). Statistically significant ($p < 0.05$) changes in relative specific activity were not detected, supporting the uniformity of mitochondrial respiratory defects across both Black and White patients at the point of amputation.

Transcriptome differences between Black and White patients with CLI

We next performed a direct comparison between tissues from Black and White patients with CLI (Figure 4A,B). These analyses revealed an upregulation of 230 genes and downregulation of 940 genes in Black patients compared to White. Reactome enrichment analysis (Figure 4C) revealed hemostasis, extracellular matrix organization, platelet regulation, and vascular wall interactions to be uniquely altered in Black patient tissues. The targets with the greatest decreases in expression in Black patient tissues are presented in Table 2 and included: pentraxin 3, long (*PTX3*), matrix metallopeptidase 9 (*MMP9*), and carbonic anhydrase XII (CA12). Targets with the greatest increases in Black patients (Table 3) were nucleoside diphosphate linked moiety X)-type motif 4 pseudogene 1 (*NUDT4P1*), ETS transcription factor ELK2A, pseudogene (*ELK2AP*), and glutamate receptor

Author Manuscript Author Manuscript Author Manuscript Author Manuscript

ionotropic, kainate 2 (*GRIK2*). We next generated heat maps for specific components of the Reactome category ‘Cell surface interactions at the vascular wall’, specifically focusing on BASIGIN interactions (Figure 4D), *PECAM1* interactions (Figure 4E), *Tie2* signaling (Figure 4F), and integrin-related interactions (Figure 4G). Overall, the solute carrier 7 family of amino acid transporters (SLC7A10, *SLC7A11*, *SLC7A5*, *SLC7A6*, *SLC7A7*, *SLC7A8*, and *SLC7A9*) demonstrated appreciable increases. *Tie2* signaling appeared largely unchanged, with general reductions noted in *PECAM1* and integrin-related interactions. Real-time quantitative reverse transcription PCR (qRT-PCR) validation of directional changes were performed for select targets (Figure 5) on limited sample numbers and verified reductions in *PTX3*, *AQP9*, and *MMP*, as well as increases in *NUDT4P1*, *GRIK2*, and *CCNG1*. A more detailed analysis of ‘traditional’ vascular growth factor signaling components from the WTSS data (Figure 6) revealed a statistically significant reduction in the expression of *Tie1* in limb muscles from Black patients with CLI, when expressed as normalized to values from White patients with CLI.

Discussion

This study represents a necessary beginning to better understand the unique characteristics of tissues from Black patients with CLI. To the best of our knowledge, this article is the first to directly compare the transcriptome from patients with CLI matched on major risk factors other than Black status. We report several key findings, including similarities in the limb skeletal muscle transcriptomes of White and Black patients compared with race-matched healthy adult tissues. These similarities largely surrounded gene expression related to cellular bioenergetics and mitochondrial function, which are known as a uniformly decreased characteristic of CLI limb muscles at amputation.[6] Direct comparisons of CLI tissues revealed a majority of genes decreased in CLI limb muscles from Black patients, as compared directly with White, at the time of amputation (230 upregulated vs 940 downregulated). The transcriptome differences between racial groups largely centered around the extracellular matrix, hemostasis, and the vascular wall. There were no observable differences in the gene expression of respiratory function genes between Black or White patients with CLI and both groups demonstrated appreciable decreases in respiratory function genes compared with their race-matched controls. Direct analysis of traditional vascular growth factors (*PDGF*, *VEGF*, *angiopoietin*) and their receptors (*Flt*, *Flk*, *Tie2*) revealed a largely race-independent gene expression profile at amputation, with the exception being decreased *Tie1* expression in tissues from Black patients with CLI. Overall, these data support two critical points: (1) race-independent transcriptome programs involving mitochondrial function and bioenergetics characterize amputation outcomes, and (2) race-dependent transcriptome differences exist and point to key changes in solute carriers (SLC) and integrins.

The diminishing effects of PAD on mitochondrial efficiency have been well studied in limb skeletal muscle.[10,11] Previous work has identified marked changes in the bioenergetic signatures of these tissues, including attenuated propensity for substrates and disproportionate levels of reactive oxygen species.[6,12,13] In this study, both Black and White patients with CLI demonstrated altered gene expression profiles contributing to mitochondrial dysfunction. These changes point to the need for development of therapeutic

Author Manuscript Author Manuscript Author Manuscript Author Manuscript

targets to improve mitochondrial function for universal patient application, regardless of race/ethnicity. General therapeutic ideas for mitochondrial support during ischemia/hypoxia currently include supportive transitioning to non-oxidative/glycolytic metabolism[14] and small peptides.[15]

We did not observe striking differences in the traditional vascular growth factor transcriptome between Black and White patients. It is possible that a differential transcriptional program for these specific factors exists in patients prior to the need for amputation, but existing control patient data do not support race-based differences in these genes at baseline (data not shown). Among the genes with the greatest observed decreases in Black patients with CLI, *Pentraxin 3*, *MMP9*, *TIMP1* are of unique interest. Pentraxin 3 is a protein produced during acute inflammatory responses in patients with atherosclerotic lesions.[16,17] Circulating Pentraxin 3 is an independent predictor of PAD in hemodialysis.[18] Decreases in limb tissues may be related to its role in tissue repair in the local environment[19] and could indicate divergent inflammatory repair/regenerative processes in the limb muscles of these patients. Decreases in *MMP9* and *TIMP1* are contextually relevant to this idea, as both have been shown to regulate skeletal muscle tissue integrity and progressive cardiovascular tissue pathology.[20,21] This is an exciting area for future therapeutic development and aligns well with the need for bioenergetic support in this space.

Increased microtubule-associated protein 1 light chain 3 beta (*MAP1LC3B*) in Black CLI tissues is worth noting. *MAP1LC3B* is essential in the autophagy pathway and its expression has been linked to the biological functions of BAG3,[22] a known regulator of limb tissue pathology in pre-clinical models of PAD.[23] Autophagy can be either protective or detrimental in vascular diseases and is often discussed specifically in a contextually dependent manner.[24] Pre-clinical work by our laboratory revealed dysfunctional autophagy as a hallmark of enhanced skeletal muscle damage during limb ischemia in a susceptible parental strain (BALB/c).[23] Autophagy is also critical for mitochondrial clearance[24,25] and undoubtedly plays a role in tissue repair/regeneration in the ischemic limb.

To the best of our knowledge, few studies have examined biological roles for lncRNA in PAD.[26,27] Increased expressions of the non-coding RNA targets *MIR503HG* and *LINC00941* highlight the potential relevance of these poorly understood components of the human genome to PAD. *MIR503HG* and *LINC00941* biologically alter cell proliferation in many disease states, including cancer, preeclampsia, and vascular remodeling,[27,28,29] are hypoxia-sensitive targets in endothelial tissues,[30] and *MIR503HG*, specifically, has been implicated in regulating *MMP9* levels in trophoblast cells in human cell lines.[28] Differential lncRNA profiles in Black patients with CLI provide an important glimpse into the potential these targets hold as unique biomarkers and targets of biological interrogation for therapeutic development.

Limitations

Limitations of these data are the noted absence of White female patients with CLI compared to Black. This underscores the concept of PAD and CLI being underrepresented in women.[31] Larger scale diagnostic studies of patients with PAD conducted in the future should be carefully designed to include similar numbers of women and men across races to better

Author Manuscript Author Manuscript Author Manuscript Author Manuscript

identify potential biochemical and/or genetic differences in these populations. While this dataset was focused on mitochondrial and mRNA-based alterations in patient populations, detailed proteomics data are a crucial and functional outcome of sequencing analyses. This is a potentially important area of investigation and analysis in future studies of patients with CLI.

Conclusion

In summary, similar reductions in the expression of genes associated with cellular bioenergetics were observed in tissues from patients with CLI regardless of race. These data further support inquiry of mitochondrial efficacy as a target for plausible therapies across both White and Black patients. The reported data also depict appreciable differences in gene expression levels in Black patients when directly compared to White patients with CLI. There are unique challenges that influence the health of represented individuals in this type of research, including factors such as access to medical care in rural settings and allostatic load. The discovered differences in the limb tissues of Black patients with CLI support further investigation into these genetic programs. Key to advancing this field of research will be larger population-based clinical trials that incorporate public health-based factors into race-related biological data collected at the tissue level. Overall, this work supports the continued study of mitochondria in CLI pathology, provides novel awareness of the contribution of lncRNAs, and establishes additional areas for investigation in Black patients with CLI.

Funding

This work was supported in part by NIH grants HL125695 (Joseph McClung), HL150003 (Brian Annex), HL141325 (Brian Annex), HL139822-01A1 (Brian Annex and Joseph McClung), and GM129074 (Feilim Mac Gabhann).

References

1. Criqui MH, Aboyans V. Epidemiology of peripheral artery disease. Circ Res 2015; 116: 1509–1526. [PubMed: 25908725]
2. Kalbaugh CA, Kucharska-Newton A, Wruck L, et al. Peripheral artery disease prevalence and incidence estimated from both outpatient and inpatient settings among Medicare fee-for-service beneficiaries in the Atherosclerosis Risk in Communities (ARIC) study. J Am Heart Assoc 2017; 6: e003796. [PubMed: 28468784]
3. Carnethon MR, Pu J, Howard G, et al. Cardiovascular Health in African Americans: A scientific statement from the American Heart Association. Circulation 2017; 136: e393–e423. [PubMed: 29061565]
4. Leeper NJ, Myers J, Zhou M, et al. Exercise capacity is the strongest predictor of mortality in patients with peripheral arterial disease. J Vasc Surg 2013; 57: 728–733. [PubMed: 23044259]
5. Allison MA, Ho E, Denenberg JO, et al. Ethnic-specific prevalence of peripheral arterial disease in the United States. Am J Prev Med 2007; 32: 328–333. [PubMed: 17383564]
6. Ryan TE, Yamaguchi DJ, Schmidt CA, et al. Extensive skeletal muscle cell mitochondriopathy distinguishes critical limb ischemia patients from claudicants. JCI Insight 2018; 3: e123235.
7. Ryan TE, Brophy P, Lin CT. Assessment of in vivo skeletal muscle mitochondrial respiratory capactiy in humans by near-infrared spectroscopy: A comparison with in situ measurements. J Physiol (Lond) 2014; 15: 3231–3241.

Author Manuscript Author Manuscript Author Manuscript Author Manuscript

8. Frezza C, Cipolat S, Scorrano L. Organelle isolation: Functional mitochondria from mouse liver, muscle, and cultured fibroblasts. Nat Protoc 2007; 2: 287–295. [PubMed: 17406588]
9. Barrientos A In vivo and in organello assessment of OXPHOS activities. Methods 2002; 26: 307–316. [PubMed: 12054921]
10. Brass EP, Hiatt WR. Acquired skeletal muscle metabolic myopathy in atherosclerotic peripheral arterial disease. Vasc Med 2000; 5: 55–59. [PubMed: 10737157]
11. Fetterman JL, Holbrook M, Westbrook DG, et al. Mitochondrial DNA damage and vascular function in patients with diabetes mellitus and atherosclerotic cardiovascular disease. Cardiovasc Diabetol 2016; 15: 53. [PubMed: 27036979]
12. Makris KI, Nella AA, Zhu Z, et al. Mitochondriopathy of peripheral arterial disease. Vascular 2007; 15: 336–343. [PubMed: 18053417]
13. Lejay A, Meyer A, Schlagowski AI, et al. Mitochondria: Mitochondrial participation in ischemia–reperfusion injury in skeletal muscle. Int J Biochem Cell Biol 2014; 50: 101–105. [PubMed: 24582887]
14. Ryan TE, Schmidt CA, Tarpey MD, et al. PFKFB3-mediated glycolysis rescues myopathic outcomes in the ischemic limb. JCI Insight 2020; 5: e139628.
15. Ryan TE, Schmidt CA, Alleman RJ, et al. Mitochondrial therapy improves limb perfusion and myopathy following hindlimb ischemia. J Mol Cell Cardiol 2016; 97: 191–196. [PubMed: 27262673]
16. Rolph MS, Zimmer S, Bottazzi B, et al. Production of the long pentraxin PTX3 in advanced atherosclerotic plaques. Arterioscler Thromb Vasc Biol 2002; 22: e10–e14. [PubMed: 12006411]
17. Deban L, Russo RC, Sironi M, et al. Regulation of leukocyte recruitment by the long pentraxin PTX3. Nat Immunol 2010; 11: 328–334. [PubMed: 20208538]
18. Zhou Y, Ni Z, Zhang J, et al. Plasma pentraxin 3 may be a better marker of peripheral artery disease in hemodialysis patients than C-reactive protein. Vasc Med 2013; 18: 85–91. [PubMed: 23609129]
19. Ristagno G, Fumagalli F, Bottazzi B, et al. Pentraxin 3 in cardiovascular disease. Front Immunol 2019; 10: 823. [PubMed: 31057548]
20. Page-McCaw A, Ewald AJ, Werb Z. Matrix metalloproteinases and the regulation of tissue remodelling. Nat Rev Mol Cell Biol 2007; 8: 221–233. [PubMed: 17318226]
21. Li H, Mittal A, Makonchuk DY, et al. Matrix metalloproteinase-9 inhibition ameliorates pathogenesis and improves skeletal muscle regeneration in muscular dystrophy. Hum Mol Genet 2009; 18: 2584–2598. [PubMed: 19401296]
22. Rodríguez AE, López-Crisosto C, Peña-Oyarzún D, et al. BAG3 regulates total MAP1LC3B protein levels through a translational but not transcriptional mechanism. Autophagy 2016; 12: 287–296. [PubMed: 26654586]
23. McClung JM, McCord TJ, Ryan TE, et al. BAG3 (Bcl-2-Associated Athanogene-3) coding variant in mice determines susceptibility to ischemic limb muscle myopathy by directing autophagy. Circulation 2017; 136: 281–296. [PubMed: 28442482]
24. Vindis C Autophagy: An emerging therapeutic target in vascular diseases. Br J Pharmacol 2015; 172: 2167–2178. [PubMed: 25537552]
25. Myers VD, McClung JM, Wang JF, et al. The multifunctional protein BAG3: A novel therapeutic target in cardiovascular disease. JACC Basic Transl Sci 2018; 3: 122–131. [PubMed: 29938246]
26. Perez-Cremades D, Cheng HS, Feinberg M.W. Noncoding RNAs in Critical Limb Ischemia. ATVB 2020; 40: 523–533.
27. Boulberdaa M, Scott E, Ballantyne M, et al. A role for the long noncoding RNA SENCR in commitment and function of endothelial cells. Mol Ther 2016; 24: 978–990. [PubMed: 26898221]
28. Cheng D, Jiang S, Chen J, et al. The increased lncRNA MIR503HG in preeclampsia modulated trophoblast cell proliferation, invasion, and migration via regulating matrix metalloproteinases and NF-κB signaling. Dis Markers 2019; 2019: 4976845. [PubMed: 31467616]
29. Luo C, Tao Y, Zhang Y, et al. Regulatory network analysis of high expressed long non-coding RNA LINC00941 in gastric cancer. Gene 2018; 662: 103–109. [PubMed: 29653230]

Author Manuscript Author Manuscript Author Manuscript Author Manuscript

30. Fiedler J, Breckwoldt K, Remmele CW, et al. Development of long noncoding RNA-based strategies to modulate tissue vascularization. J Am Coll Cardiol 2015; 66: 2005–2015. [PubMed: 26516004]

31. Mentias A, Vaughan-Sarrazin M. Sex differences in management and outcomes of critical limb ischemia in the Medicare population. Circ Cardiovasc Interv 2020; 13: e009459. [PubMed: 33079598]

Author Manuscript Author Manuscript Author Manuscript Author Manuscript

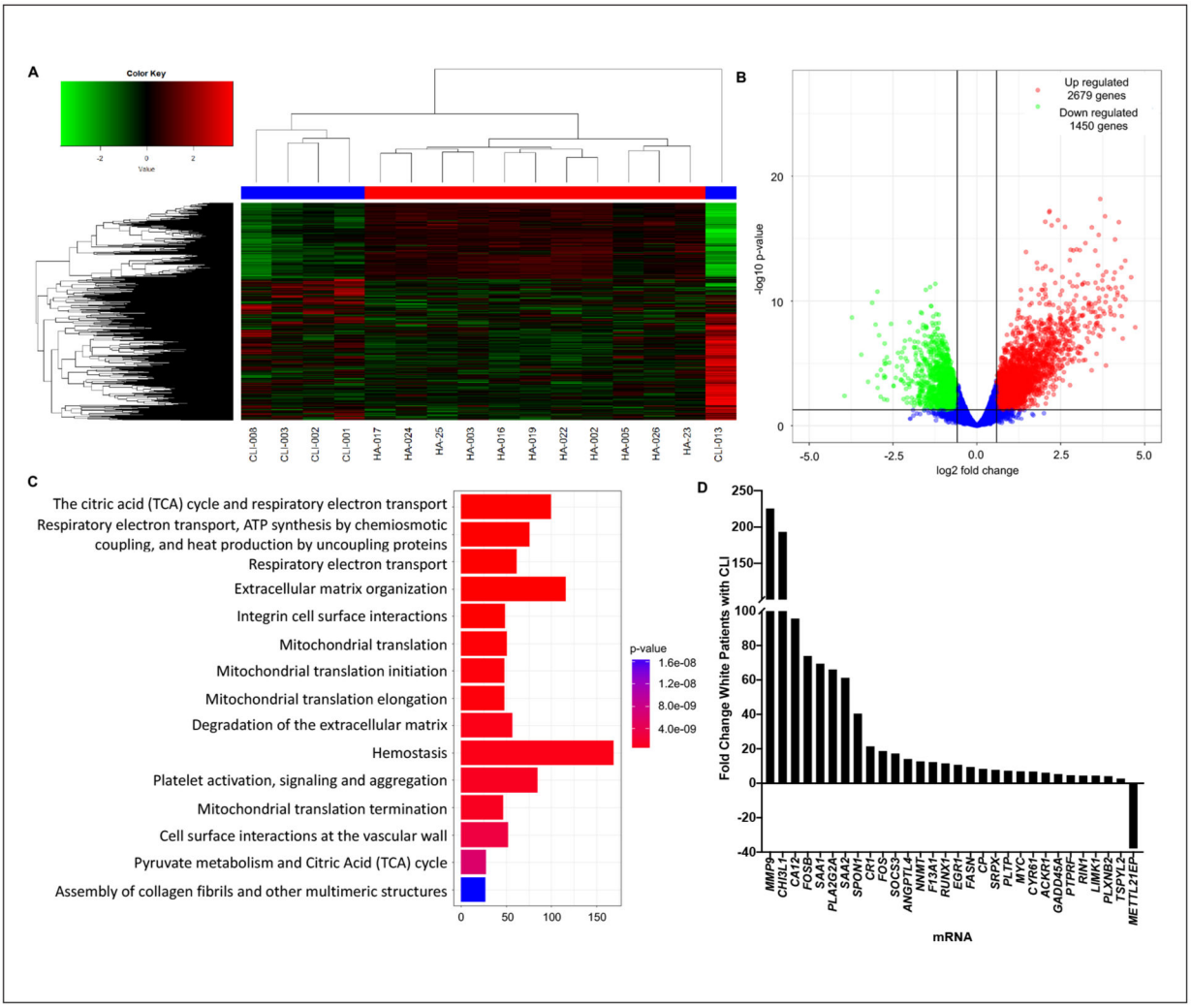

Figure 1.

RNA sequencing in muscle biopsy specimens from White patients with CLI. Limb muscle biopsies were acquired from White HA or patients with CLI and WTSS was performed. (A) Heatmap of all differentially expressed genes. (B) Volcano plot representing differential gene expression between HA and CLI. (C) Reactome enrichment analysis indicating the most significant gene expression changes were related to bioenergetics. (D) Histogram of top 30 gene targets identified by WTSS of limb skeletal muscle of White patients with CLI (n = 5) compared to White controls (HA, n = 11).

List sorted by significance (p-value) and the top 30 targets are represented, either decreased fold change (–) or increased. Fold change representative of target message counts.

CLI, critical limb ischemia; HA, healthy adult; WTSS, whole transcriptome shotgun sequencing.

Author Manuscript
Author Manuscript
Author Manuscript
Author Manuscript

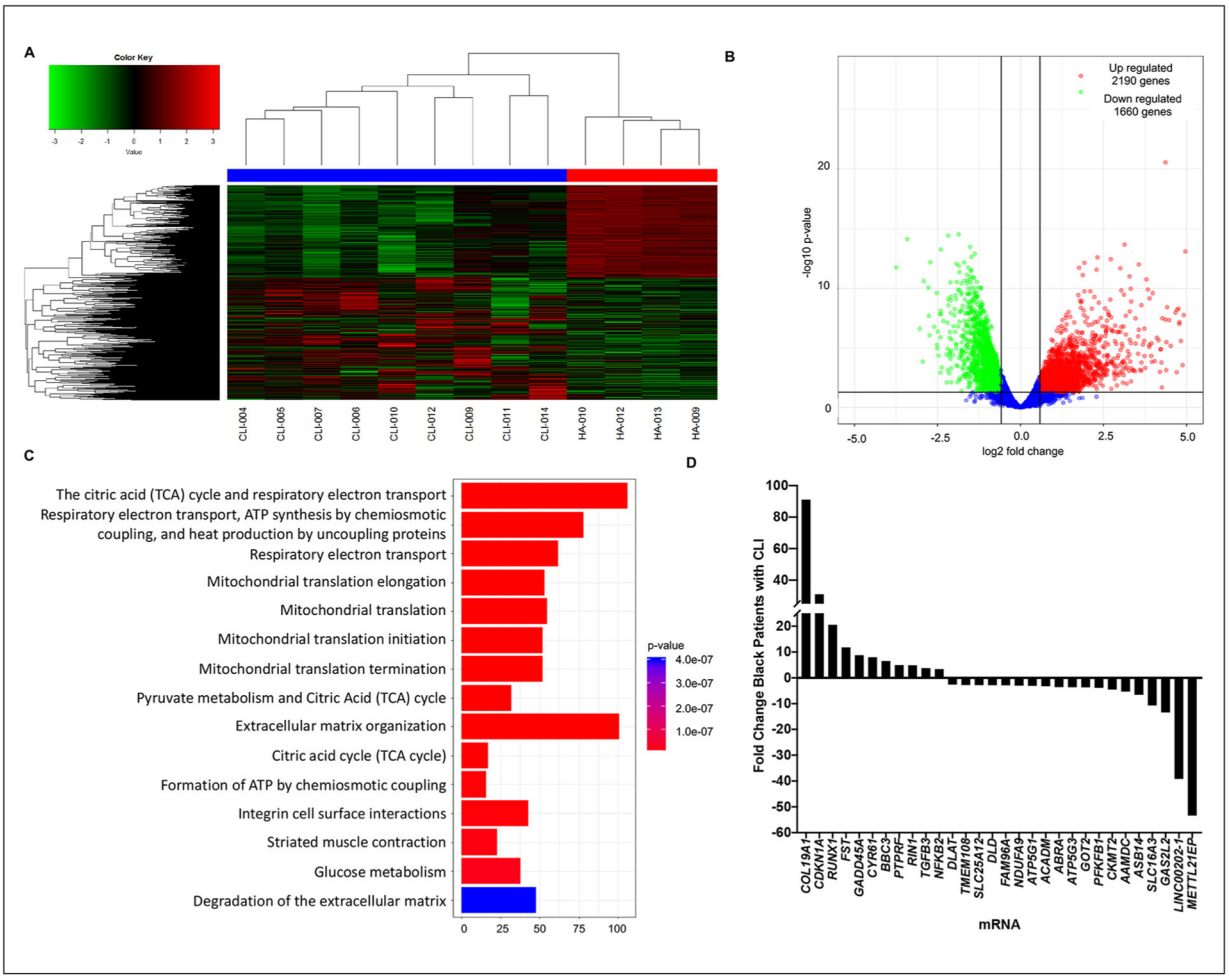

Figure 2.

RNA sequencing in muscle biopsy specimens from Black patients with CLI. Limb muscle biopsies were acquired from Black HA or CLI patients and WTSS was performed. (A) Heatmap of all differentially expressed genes. (B) Volcano plot representing differential gene expression between HA and CLI. (C) Reactome enrichment analysis indicating the most significant gene expression changes were related to bioenergetics. (D) Histogram of top 30 gene targets identified by WTSS of limb skeletal muscle of Black patients with CLI ($n = 9$) compared to Black controls (HA, $n = 4$).

List sorted by significance (p-value) and the top 30 targets are represented, either decreased fold change (–) or increased. Fold change representative of target message counts.

CLI, critical limb ischemia; HA, healthy adult; WTSS, whole transcriptome shotgun sequencing.

Author Manuscript Author Manuscript Author Manuscript Author Manuscript

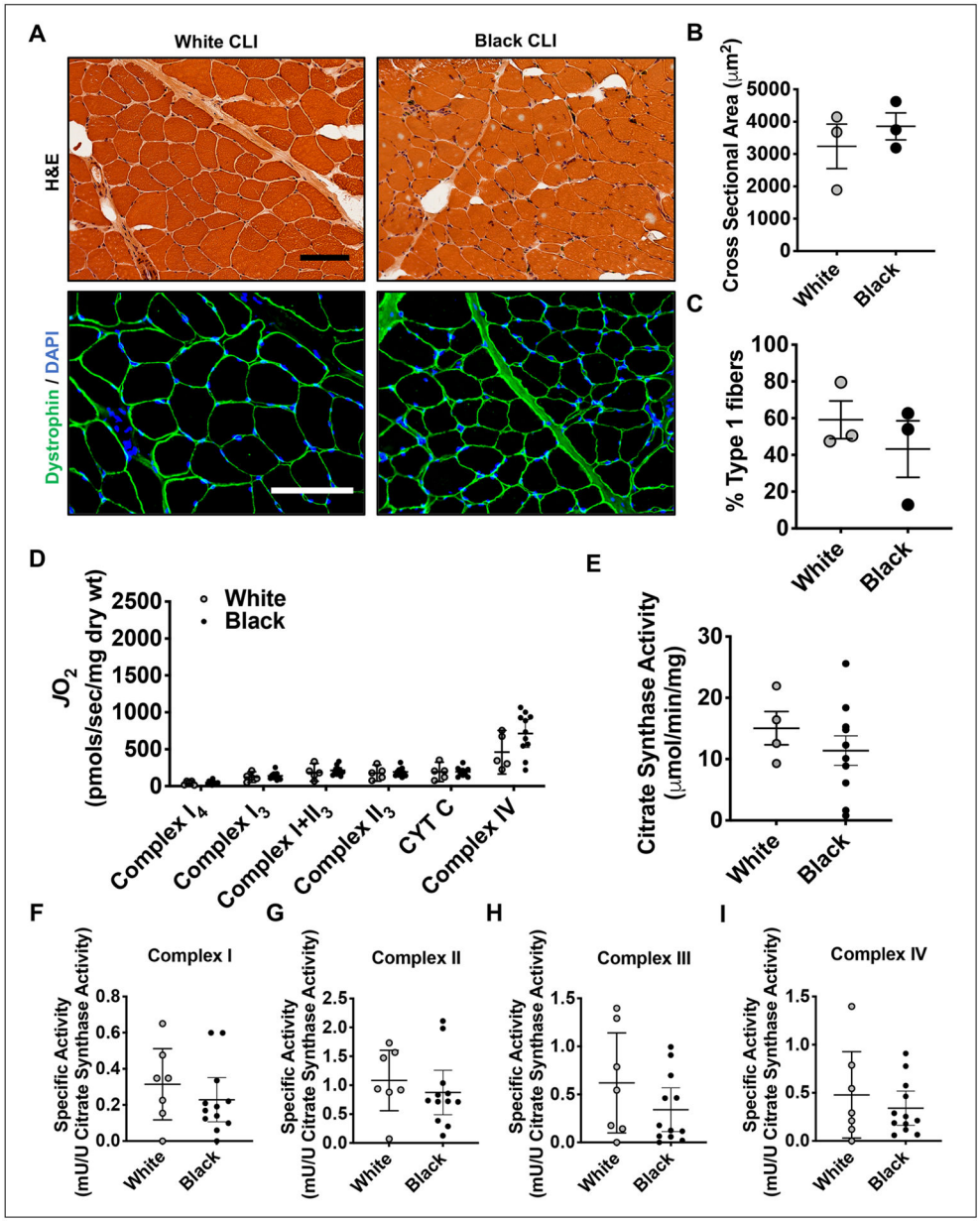

Figure 3.

Histological and mitochondrial phenotyping. Skeletal muscle biopsy specimens were obtained from the tibialis anterior of White and Black patients with CLI. (A) Histological (H&E staining) assessment and immunofluorescent staining for dystrophin confirms that samples obtained were not from necrotic regions within the limb. (B) Quantification of mean myofiber cross-sectional area. (C) Quantification of the percentage of Type I myofibers in each group. Scale bars indicate 200 μm. (D) Skeletal muscle mitochondrial respiratory function was measured in permeabilized myofiber samples collected at amputation from White and Black patients. No obvious alterations were observed in Complex I_3 (state 3), I + II, II, and IV-supported oxygen consumption (error bars in panel D are 95% CI) ($n = 4$ for White, $n = 10$ for Black). Mitochondrial content was assessed by citrate synthase activity (E)

Author Manuscript Author Manuscript Author Manuscript Author Manuscript

(n = 7 for White, n = 10 for Black) indicating that mitochondrial content was not different. (F–I) Biochemical enzyme assays of muscle lysates were performed to further dissect changes in the mitochondrial electron transport system. These assays indicate no alterations in specific activities (normalized for citrate synthase activity) in Complexes I, II, and IV in patients with CLI (n = 7 for White, n = 12 for Black).

Error bars represent the mean and SEM.

CLI, critical limb ischemia; CYT, cytochrome; DAPI, DAPI reagent; H&E, hematoxylin and eosin.

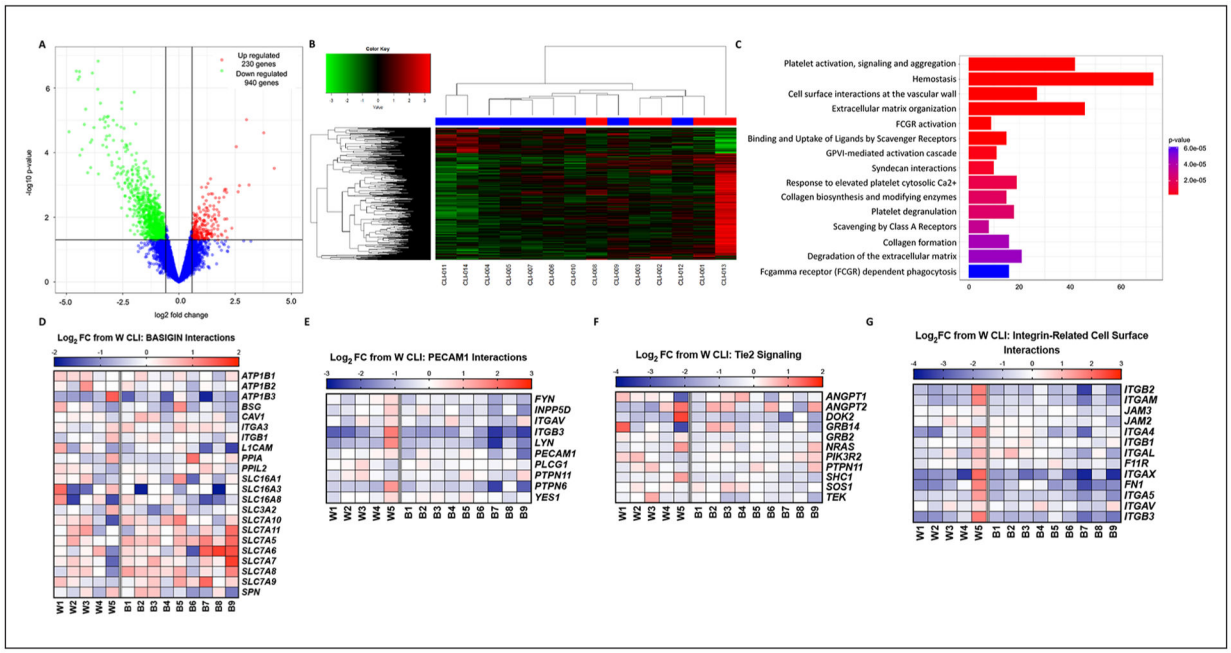

Figure 4.

RNA sequencing comparison between muscle biopsy specimens from White and Black patients with CLI. Limb muscle biopsies were acquired from White and Black patients with CLI and WTSS was performed. (A) Heatmap of all differentially expressed genes between White and Black patients. (B) Volcano plot representing differential gene expression between White and Black patients. (C) Reactome enrichment analysis indicating the most significant gene expression changes were related to hemostasis, the vascular wall, and the extracellular matrix. (D–G) Heatmap of gene expression differences [log2 (fold change from HA)] for the Reactome terms and genes associated with BASIGIN interactions, *PECAM1* interactions, *Tie2* signaling, and integrin-related cell-surface interactions, respectively. CLI, critical limb ischemia; FC, fold change; HA, healthy adult; WTSS, whole transcriptome shotgun sequencing.

Author Manuscript Author Manuscript Author Manuscript Author Manuscript

Author Manuscript Author Manuscript Author Manuscript Author Manuscript

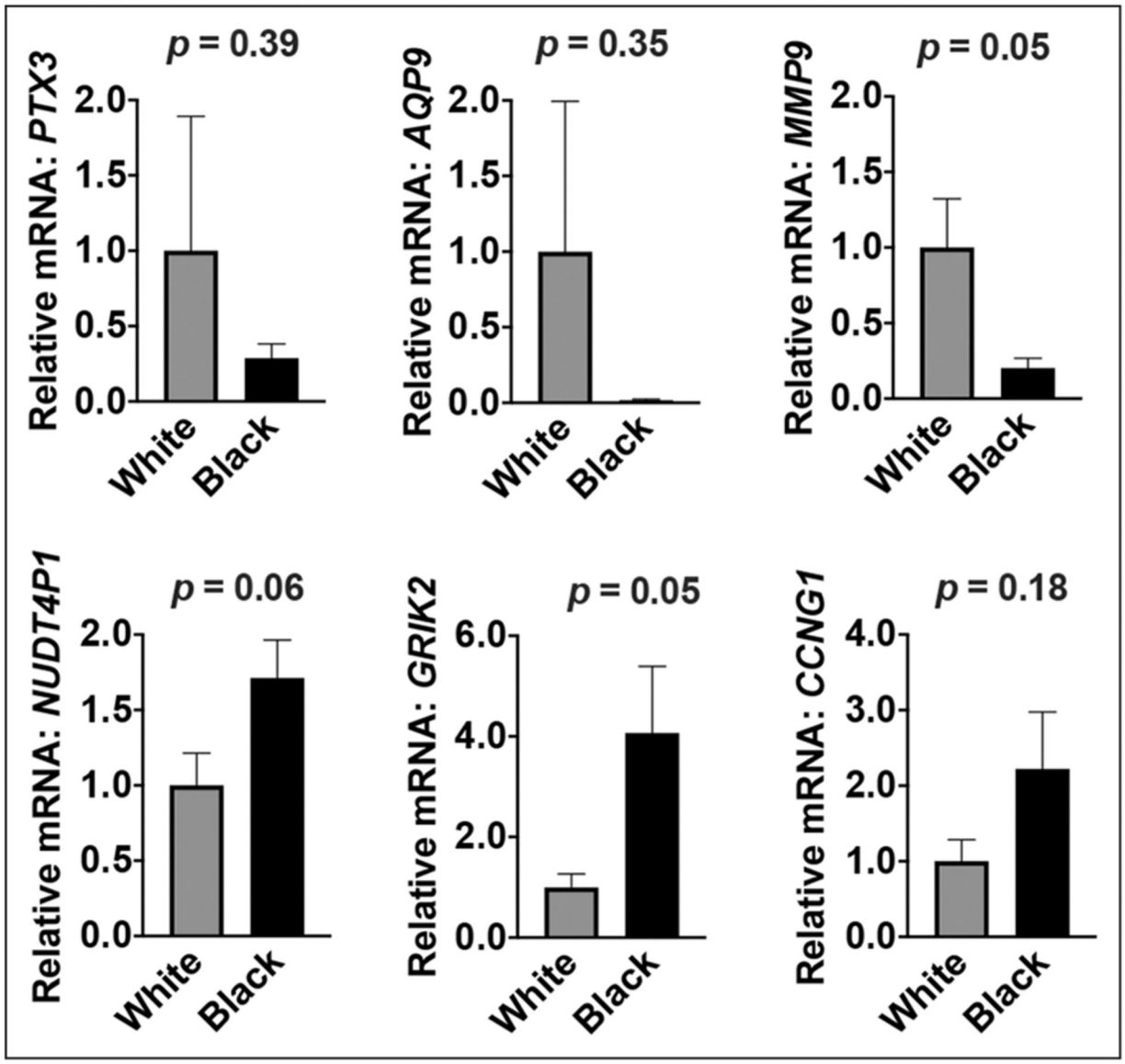

Figure 5.

qRT-PCR validation of directional changes of selected identified genes.

Values are presented as mean ± SE; *p*-values are provided where applicable.

qRT-PCR, Real-Time Quantitative PCR.

Author Manuscript Author Manuscript Author Manuscript Author Manuscript

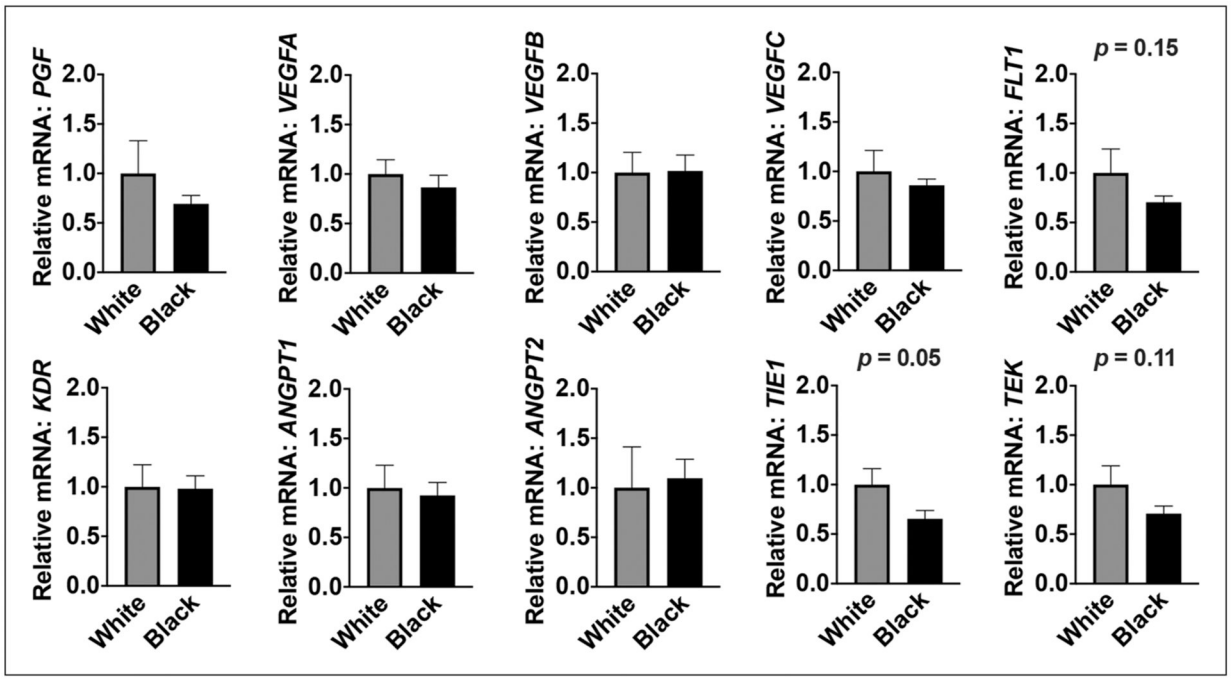

Figure 6.

WTSS comparison of traditional vascular growth factors and receptors between White and Black patients with CLI. Values are presented as mean ± SE; *p*-values are provided where applicable.

CLI, critical limb ischemia; HA, healthy adult; WTSS, whole transcriptome shotgun sequencing

Author Manuscript Author Manuscript Author Manuscript Author Manuscript

Vasc Med. Author manuscript; available in PMC 2021 June 25.

Table 1.

Patient characteristics.

Characteristic	HA-W (*n* = 11)	CLI-W (*n* = 5)	HA-B (*n* = 4)	CLI-B (*n* = 9)
Mean age, years (SD)	57 (6.6)	59 (8.9)	57 (3.7)	69 (10.1)
Female sex, no. (%)	7 (64)	0 (0)	4 (100)	6 (67)
Medical history, no. (%)				
Diabetes mellitus type I or II	0 (0)	3 (60)	0 (0)	7 (78)
Hypertension	0 (0)	5 (100)	0 (0)	6 (67)
Hyperlipidemia	0 (0)	1 (20)	0 (0)	3 (33)
CAD	0 (0)	0 (0)	0 (0)	4 (44)
Renal disease	0 (0)	2 (40)	0 (0)	5 (56)
Tobacco use, no. (%)				
Former smoker	0 (0)	2 (40)	0 (0)	8 (88)
Current smoker	0 (0)	3 (60)	0 (0)	1 (11)
Family history of CAD, no. (%)	0 (0)	3 (60)	0 (0)	5 (56)
ABI at amputation (mean ± SE) (*n*)	NA	0.43 ± 0.21 3 (2 NC)	NA	0.31 ± 0.13 5 (4 NC)
Previous revascularization, no. (%)	NA	3 (60)	NA	4 (44)

ABI, ankle–brachial index; ABI NC, non-compressible at the time of amputation; Avg, average; B, Black patient; CAD, coronary artery disease; CLI, critical limb ischemia; HA, healthy adult; W, White patient.

Author Manuscript Author Manuscript Author Manuscript Author Manuscript

Vasc Med. Author manuscript; available in PMC 2021 June 25.

Table 2.

Gene list of decreased expression in limb skeletal muscle from Black ($n = 9$) and White ($n = 5$) patients with CLI.

Gene symbol	Gene name	Fold change (from CLI-W)	*p*-value	FDR
PTX3	pentraxin 3, long	−36.48	0.00000012	0.0008592
FBP1	fructose-1,6-bisphosphatase 1	−12.08	0.00000015	0.0008592
CA12	carbonic anhydrase XII	−23.65	0.00000030	0.0008592
ALPL	alkaline phosphatase, liver/bone/kidney	−21.46	0.00000031	0.0008592
ANPEP	alanyl (membrane) aminopeptidase	−14.46	0.00000034	0.0008592
AQP9	aquaporin 9	−21.45	0.00000045	0.0009670
CEMIP	cell migration inducing protein, hyaluronan binding	−22.37	0.00000054	0.0010137
THBS1	thrombospondin 1	−12.24	0.00000109	0.0018099
FADS1	fatty acid desaturase 1	−3.98	0.00000134	0.00200833
MMP9	matrix metallopeptidase 9	−32.93	0.00000263	0.0033987
SLC16A3	solute carrier family 16 (monocarboxylate transporter), member 3	−5.85	0.00000281	0.00339869
SERPINE1	serpin peptidase inhibitor, clade E (nexin, plasminogen activator inhibitor type 1), member 1	−11.28	0.00000295	0.00339869
SRGN	serglycin	−5.82	0.00000435	0.0045012
ST14	suppression of tumorigenicity 14 (colon carcinoma)	−17.74	0.00000452	0.0045012
ADAMTS4	ADAM metallopeptidase with thrombospondin type 1 motif, 4	−8.87	0.00000747	0.00658073
CLIC6	chloride intracellular channel 6	−9.92	0.00000779	0.00658073
PLAUR	plasminogen activator, urokinase receptor	−9.16	0.00000792	0.00658073
TIMP1	TIMP metallopeptidase inhibitor 1	−10.37	0.00000916	0.00672507
STC1	stanniocalcin 1	−11.44	0.00000937	0.00672507
CD52	CD52 molecule	−7.55	0.00000990	0.00672507

List generated from WTSS data, sorted by significance (*p*-value), and the top 20 targets represented.

Fold change representative of target message counts.

CLI, critical limb ischemia; FDR, false discovery rate; W, White; WTSS, whole transcriptome shotgun sequencing.

Author Manuscript Author Manuscript Author Manuscript Author Manuscript

Vasc Med. Author manuscript; available in PMC 2021 June 25.

Table 3.

Gene list of increased expression in limb skeletal muscle from Black ($n = 9$) and White ($n = 5$) patients with CLI.

Gene symbol	Gene name	Fold change (from CLI-W)	*p*-value	FDR
NUDT4P1	nudix (nucleoside diphosphate linked moiety X)-type motif 4 pseudogene 1	663.77	0.00000033	0.00085925
LRRC3B	leucine rich repeat containing 3B	8.01	0.00000950	0.00672507
GRIK2	glutamate receptor, ionotropic, kainate 2	13.66	0.00002419	0.01096150
LGALS17A	Charcot-Leyden crystal protein pseudogene	5.86	0.00006515	0.02115284
ELK2AP	ELK2A, member of ETS oncogene family, pseudogene	18.78	0.00030454	0.06413270
KCNQ4	potassium channel, voltage gated KQT-like subfamily Q, member 4	2.65	0.00064132	0.09400990
CCNG1	cyclin G1	2.45	0.00090062	0.11608667
IGLL5	immunoglobulin lambda-like polypeptide 5	8.67	0.00099507	0.12195291
IGJ	NA	6.45	0.00104779	0.12737076
CEACAM19	carcinoembryonic antigen-related cell adhesion molecule 19	2.00	0.00117680	0.13575224
PDE4D	phosphodiesterase 4D, cAMP-specific	2.32	0.00118030	0.13575224
MAP1LC3B2	microtubule-associated protein 1 light chain 3 beta 2	4.09	0.00135863	0.14614533
SH2D1B	SH2 domain containing 1B	4.27	0.00137164	0.14649077
PCDH8	protocadherin 8	4.06	0.00154218	0.15793572
FCRLA	Fc receptor-like A	6.17	0.00162094	0.16375837
MIR503HG	MIR503 host gene	4.35	0.00169218	0.16755900
ACADL	acyl-CoA dehydrogenase, long chain	2.69	0.00186607	0.17548098
LINC00941	long intergenic non-protein coding RNA 941	2.82	0.00188536	0.17618670
DEPDC7	DEP domain containing 7	2.48	0.00191760	0.17808665
PREPL	prolyl endopeptidase-like	2.08	0.00235309	0.19262850

List generated from WTSS data, sorted by significance (*p*-value), and the top 20 targets represented.

Fold change representative of target message counts.

FDR, false discovery rate; WTSS, whole transcriptome shotgun sequencing.